Research Article

Propellants, Explosives, Pyrotechnics

doi.org/10.1002/prep.202100047

Thermally Stable and Low-Sensitive Aluminized Explosives with Improved Detonation Performance

Songwei He,[a] Kaiyuan Tan,[a] Qingguan Song,[a] Guansong He,[a] and Wei Cao*[a]

Abstract: Two new types of aluminized explosives TATB/HMX/Al and LLM-105/Al were formulated and compared with the formerly reported TATB/Al explosives in terms of thermal stability, mechanical sensitivity, and detonation performance. Firstly, the heat of the explosion was measured and two formulations were selected as the investigated samples. Next the thermal stability was studied by simultaneous thermogravimetric analysis/differential scanning calorimetry (TGA/DSC) and thermal cook-off tests. Then the impact and friction sensitivity were measured, and finally the detonation performance was characterized by cylinder tests and particle velocity measurements of the detonation reaction zone. From the calorimetric data, the new types of explosives increase the heat of the explosion significantly. In terms of thermal stability, LLM-105/Al = 65/30 is more stable than TATB/HMX/Al = 50/15/30, but both of them are inferior to TATB/Al = 70/25. The impact sensitivity of the two new explosives is higher than that of TATB/Al = 70/25, and all of the samples are insensitive to friction. For detonation performance, both of the two new samples are superior to TATB/Al = 70/25, and LLM-105/Al = 65/30 exhibits the best performance that it has the highest Gurney energy, detonation velocity, and detonation pressure. Conclusions about how to use those aluminized explosives to generate optimal effects are drawn.

Keywords: thermal stability · detonation performance · low sensitivity · aluminized explosive · LLM-105

1 Introduction

Aluminized explosives have been widely used in ammunitions due to their high blast and incendiary effects [1]. The aluminum powders in explosives react with detonation products and environmental gases to release large amounts of heat, which increases the heat of detonation and damage to the target [2–4]. On the one hand, higher performance has always been a prime requirement in the field of research and development of explosives and the quest for the most powerful high explosives still continues and never ends. On the other hand, many catastrophic explosions resulted from unintentional initiation of munitions by impact, shock, and fire. Thus, in modern ordance, there are strong requirements for explosives having both good stability and better performance. However, these requirements are somewhat mutually exclusive. The explosives having good insensitiveness usually exhibit poorer explosive performance and vice versa [5].

TATB (2,4,6-triamino-1,3,5-trinitrobenzene, $C_6H_6N_6O_6$) is a reasonably powerful high explosive (HE) whose thermal and shock stability is considerably greater than that of any other known material of comparable energy [6]. TATB-based aluminized explosives have exhibited the highly thermal stability, and high detonation performance [7]. However, the TATB/Al/binder formulations reported in [7] don't meet the requirement for efficient damage. Research is ongoing in the search for more powerful aluminized explosives with good thermal, impact, and shock stability. Meanwhile, several dozen compounds classified as thermally stable explosives or insensitive high explosives (IHEs) have been synthesized [5,8–10]. Among them, LLM-105 (2,6-diamino-3,5-dinitropyrazine-1-oxide, $C_4H_4N_6O_5$) is a promising IHE whose calculated energy content is ~85% that of HMX (octahydro-1,3,5,7-tetranitro-1,3,5,7-tetrazocine, $C_4H_8N_8O_8$) and ~115% that of TATB [11–13]. It also exhibits excellent thermal stability and be insensitive to shock, spark, friction, and impact [14–18].

Thus, in order to improve the detonation performance of the highly thermally stable TATB/Al/polyvinyl butyral (PVB) explosives reported in [4], two methods were chosen in this work: one is the total replacement of TATB with LLM-105, and the other is the partial replacement of TATB with HMX. Then we studied the thermal stability, mechanical sensitivity, and detonation performance of those explosives, expecting to get the thermally stable and low-sensitive aluminized explosives with improved detonation performance.

[a] *S. He, K. Tan, Q. Song, G. He, W. Cao*
Institute of Chemical Materials, China Academy of Engineering Physics
P.O. Box 919-318, Mianyang, Sichuan 621999, China
**e-mail: weicao@caep.cn*

2 Experimental Section

2.1 Explosive Samples Preparation

TATB (purity 99%, the particle size of 8–25 μm with mean particle size ~15 μm) and LLM-105 (purity 99%, polyhedral structure with mean particle size ~25 μm) were produced by Institute of Chemical Materials, China Academy of Engineering Physics. HMX (purity 99%, particle size of 3–20 μm with mean particle size ~10 μm) was produced by Gansu Yinguang Chemical Industry Group Co., Ltd., China. Spherical aluminum powders (purity 99.8%, particle size about 5–10 μm) were provided by Angang Group Aluminum Powder Co., Ltd., China. The binder of fluorine resin was provided by Zhonghao Chenguang Chemical Industry Co., Ltd., China. Other chemical reagents, such as ethyl acetate and butyl acetate were commercial analytical pure (AR) used as solvents and without further treatment.

The weight percent of binder in all formulations was set at 5% and was omitted in the following text. The TATB/HMX/Al and LLM-105/Al explosive formulations were produced by a non-aqueous solvent granulation method, and then the molding powders were dried at 60 °C for 24 h to eliminate solvent. Next, the cylindrical charges were uniaxially pressed in a steel mold with desired geometries under a pressure of 240 MPa. The densities (ρ_0) of the obtained charges ranged from 1.98 to 2.04 g/cm^3. The morphology of molding powders was imaged by a scanning electron microscopy (SEM) and shown in Figure 1.

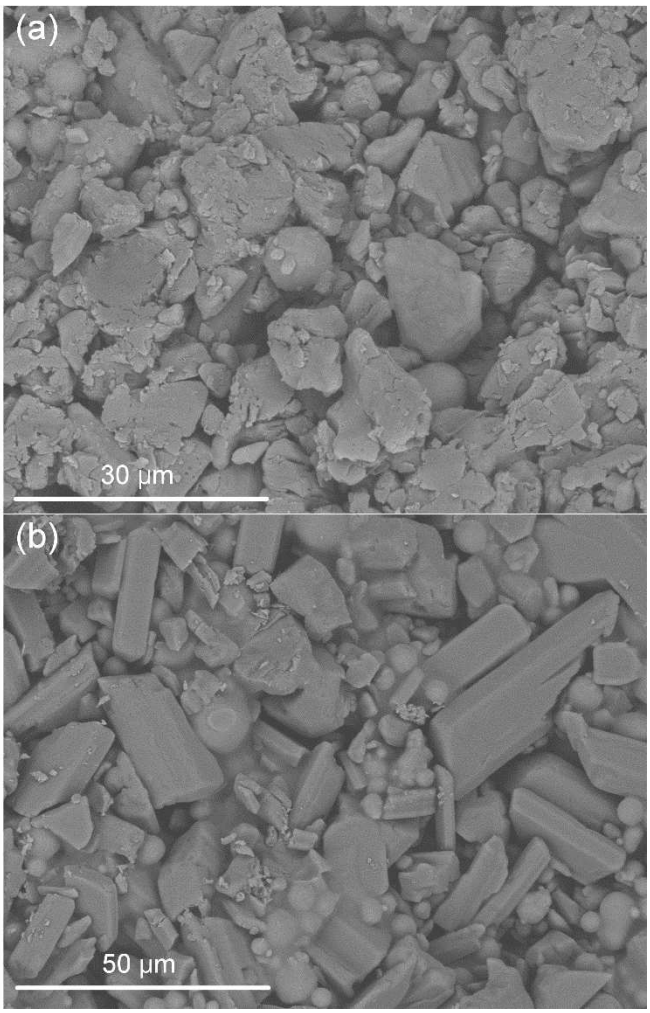

Figure 1. SEM images of molding powders for (a) TATB/HMX/Al = 45/20/30 and (b) LLM-105/Al = 65/30.

2.2 Test Methods

First, the calorimetric heat of explosion (Q_c) of several tested composites was measured by the adiabatic calorimetry method. The cylindrical bomb, made of stainless steel, has a volume of 5.0 L. A cylindrical charge with mass of ~30 g and diameter 25 mm was initiated by a Φ25 mm × 10 mm HMX-based booster (HMX/binder = 95/5, $\rho_0 = 1.860 \pm 0.002$ g/cm^3) and a Chinese commercial No. 8 detonators in 0.1 MPa nitrogen atmosphere. To calculate the detonation heat of the sample charge, the measured total heat is subtracted by the heat released from the booster (5729.68 J/g) and detonator (4422.67 J). Two formulations representing TATB/HMX/Al and LLM-105/Al were selected for the following tests.

Next, two methods were used to study the thermal stability of samples. First, the simultaneous thermogravimetric analysis/differential scanning calorimeter (TGA/DSC) was recorded on a Mettler-Toledo TGA/DSC 2 instrument. Samples of 2–3 mg were heated from 50 to 750 °C in a sealed high-pressure steel crucible at a heating rate of 10 °C/min. The reaction was studied in a nitrogen atmosphere with a constant flow rate of 30 ml/min. Second, the thermal cook-off experiment was conducted by using a cylindrical charge of Φ60 × 120 mm (two Φ60 × 60 mm cylinders). The cylinders were charged in a steel vessel (Φ68 × 128 mm, 4 mm in thickness) and heated by a heating jacket. The temperature was programmed with a thermocouple fixed on the shell of the vessel. The charge was heated at a rate of 3 K/min from room temperature to a temperature when the thermal runaway of the explosive took place. A pressure sensor was installed 2 m away to measure the overpressure of shock waves.

The mechanical sensitivity tests include impact and friction sensitivity tests. The impact sensitivity was surveyed by BAM Fallhammer test and the friction sensitivity was surveyed by BAM friction test [19].

The detonation performance tests incorporate cylinder tests and detonation reaction zone measurements. The cylinder test was performed to determine the explosives' ability to accelerate metal and to measure the detonation velocity simultaneously as shown in Figure 2. In the cylinder test, twelve pressed cylinders with the dimensions of Φ25 mm × 25 mm were stacked in a line and inserted into

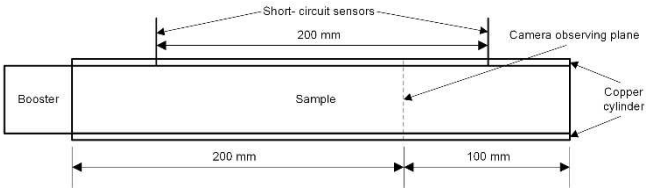

Figure 2. Schematic of cylinder test.

an oxygen-free copper tube with the dimensions of 300 mm length, 25 mm inner diameter, and 30 mm outer diameter. A Φ25 mm × 25 mm booster (HMX/binder = 95/5, $\rho_0 = 1.860 \pm 0.002$ g/cm^3) was used to initiate the explosive at one end. The radial motion of the cylinder wall was measured in a plane perpendicular to the cylinder axis and 200 mm from the booster end. The motion was recorded by a high-speed rotating mirror streak camera (writing speed 1.5 mm/μs), using an argon bomb as an illuminator. The experimental detonation velocity *D* of explosives was measured simultaneously during the cylinder test using the short-circuit sensors method [20].

The detonation reaction zone parameters were obtained from the interface particle velocity history between a detonating explosive and a lithium fluoride (LiF) transparent window as shown in Figure 3. A Φ50 × 50 mm cylindrical sample charge was detonated at one end by a Φ50 × 20 mm HMX-based booster (HMX/binder = 95/5, $\rho_0 = 1.860 \pm 0.002$ g/cm^3) and a plane wave lens. The plane wave lens initiated the booster that provided ~36 GPa pressure into the sample charge. A Φ50 × 50 mm sample charge was used to reach a stable detonation state. A Φ20 × 10 mm LiF window was mounted at the center of the other end of the sample charge, and a 0.6-μm-thick aluminum foil was deposited on the window face next to the explosive to provide a reflective surface. The laser beam was vertically focused on the center of the foil, and the interface particle velocity history was recorded by a photonic Doppler velocimetry (PDV) system with nanosecond time scales.

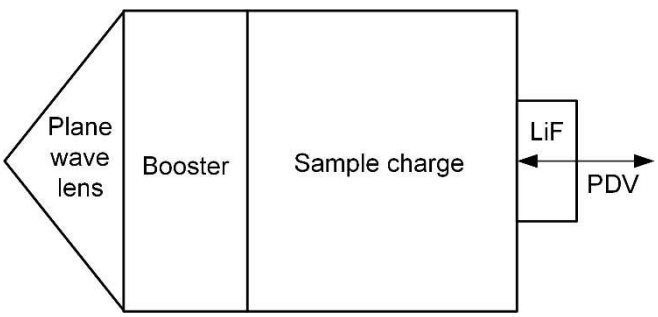

Figure 3. Geometry of the interface particle velocity measurement.

3 Results and Discussions

3.1 Calorimetric Heat of Explosion

Results of calorimetric heat of explosion of four new formulations and two reference formulations in [7] are illustrated in Figure 4. The results are the average of at least two measurements with relative errors less than 4%. It is apparent that with the substitution of TATB for HMX or LLM-105, the calorimetric heat of explosion increased. Two representative formulations TATB/HMX/Al = 50/15/30 and LLM-105/Al = 65/30 have about the same calorimetric heat of explosion (7236 and 7212 J/g, respectively), which were selected to study their thermal stability, sensitivity, and detonation performance in the following.

3.2 Thermal Stability

3.2.1 TGA-DSC

The TGA/DSC curves of two selected formulations are shown in Figure 5. For TATB/HMX/Al = 50/15/30, a typical thermal decomposition curve for a ternary system was observed. The first and second exothermic peaks at 281.6 °C and 382 °C correspond to the thermal decomposition of HMX [21] and TATB [6], respectively. The endothermic peak at 664 °C represents the melting of aluminum powders. Similarly for LLM-105/Al = 65/30, a typical thermal decomposition curve for a binary system was illustrated. The exothermic peak at 354 °C and the endothermic peak at 663 °C

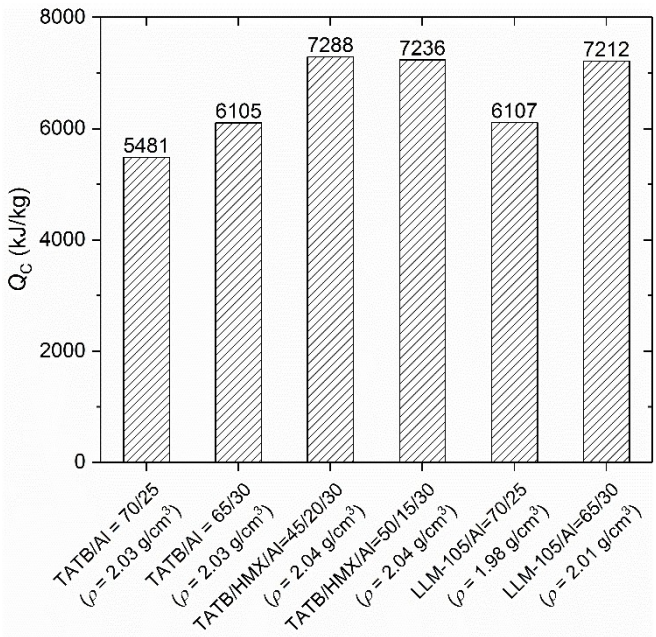

Figure 4. Calorimetric heat of the explosion.

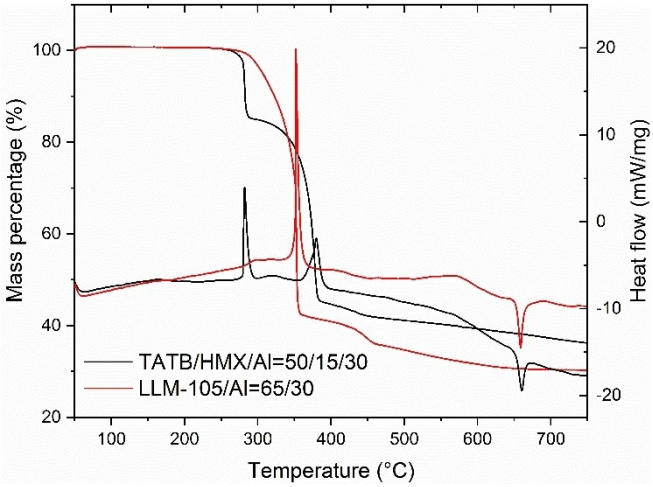

Figure 5. TGA/DSC curves of samples.

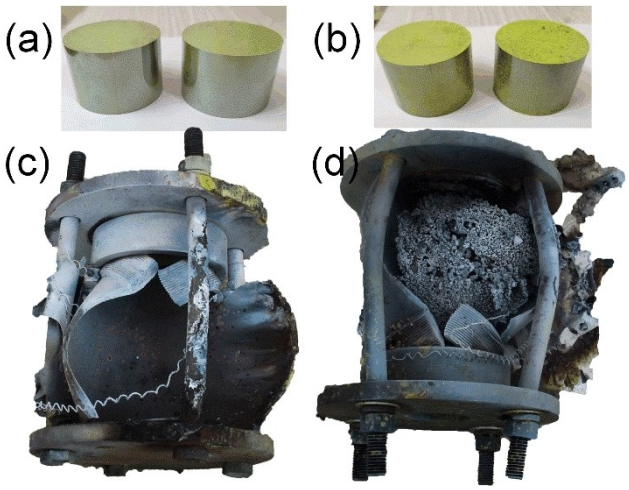

Figure 6. Samples before tests and vessels after tests: (a,c) TATB/HMX/Al = 45/20/30 and (b,d) LLM-105/Al = 65/30.

denote the thermal decomposition of LLM-105 [22] and melting of aluminum, respectively. Compared to the thermal decomposition peaks of those pure explosives, aluminum exhibits no effect on the thermal stability of those explosives in formulations. Obviously, LLM-105/Al = 65/30 has a high thermal decomposition peak and is better in thermal stability between the two formulations.

3.2.2 Thermal Cook-Off

The cook-off test results of the two investigated samples and a reference sample (TATB/Al = 70/25) are summarized in Table 1. Among those three explosives, TATB/HMX/Al = 50/15/30 has the lowest runaway temperature and LLM-105/Al = 65/30 has the medial runaway temperature, which indicates that the thermal stability of those two investigated samples is inferior to the reference sample. Nevertheless, the type of response to the cook-off tests for all samples was "burning" as shown in Figure 6, and no shock wave overpressure was detected. Thus, the violence of reaction in confined cook-off is relatively low, which complies with the request of low vulnerability and proves the thermal stability of those explosives.

3.3 Mechanical Sensitivity

The impact and friction sensitivity of samples is listed in Table 2. The limiting impact energy characterizing the impact sensitivity of a substance is defined as the lowest impact energy at which the result "explosion" is obtained at least one out of at least six trials. The impact energy used is calculated from the mass of the drop weight and the fall height. LLM-105/Al = 65/30 has the lowest limiting impact energy while TATB/Al = 70/25 has the highest value as shown in Table 2, which means that TATB/Al has the lowest impact sensitivity and LLM-105/Al is the most sensitive to impact among the three explosives. For all the three explosive formulations in the friction sensitivity test, the result

Table 1. Cook-off results of explosives under the heating rate of 3 °C/min.

Explosive	Runaway temperature (°C)	Type of response	Shock wave overpressure
TATB/HMX/Al = 50/15/30	208	Burning	–
LLM-105/Al = 65/30	285	Burning	–
TATB/Al = 70/25	310	Burning	–

Table 2. Mechanical sensitivity of explosives.

Explosive	Limiting impact energy (J)	Limiting friction load (N)
TATB/HMX/Al = 50/15/30	37.5	360
LLM-105/Al = 65/30	20	360
TATB/Al = 70/25	55	360

"decomposition" or "no reaction" occurs under the maximum load of 360 N in all six trials, which indicates all the three substances are insensitive to friction.

3.4 Detonation Performance

3.4.1 Cylinder Test

The exemplary negative film of the copper tube driven by the detonation products is shown in Figure 7. The film was processed to determine the tube velocity as described in [23]. The total velocity (u_L) of the tube obtained from both the radial velocity of the tube and the detonation velocity (D) was drawn in Figure 8 against the relative volume of detonation products.

The acceleration ability of an explosive can be described by the so-called Gurney energy E_G, which is defined as a sum of the kinetic energy of the metal shell fragments and the detonation products. For cylindrical geometries, the Gurney energy is expressed as

$$E_G = (\mu + 1/2)u_L{}^2/2, \quad (1)$$

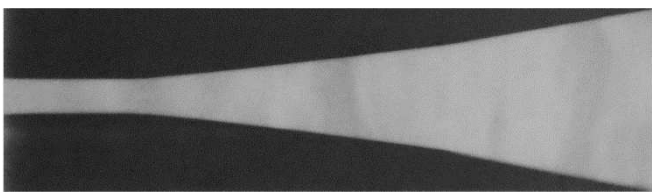

Figure 7. Exemplary film of the copper tube driven by the detonation products.

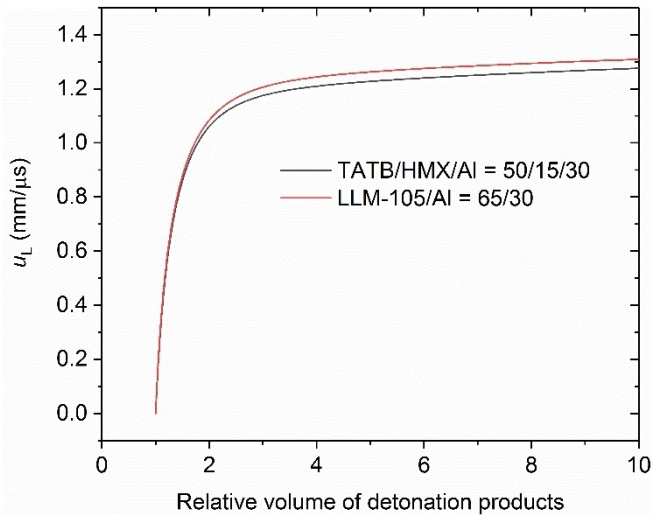

Figure 8. Variation of the tube wall velocity with the relative volume of detonation products.

where μ is the ratio of the cylinder to the explosive per unit of length. The obtained results are presented in Figure 9 with the results of TATB/Al = 70/25.

Practically, the final values of the wall velocity and Gurney energy before the disruption of the copper tube (~3 times initial diameter) are the most significant. From Figures 8 and 9, the profiles exhibit an identical trend that, with the increasing relative volume of detonation products, LLM-105/Al = 65/30 has a better metal acceleration ability than TATB/HMX/Al = 50/15/30. When compared with TATB/Al = 70/25 as shown in Figure 9, LLM-105/Al = 65/30 and TATB/HMX/Al = 50/15/30 accelerate copper tubes faster at the initial expanding process and have higher Gurney energy before the disrupture of tubes. Values of the copper tube velocity and Gurney energy at a relative tube volume of 9 are listed in Table 3.

3.4.2 Detonation Reaction Zone

The Zel'dovich-Neumann-Döring (ZND) detonation model assumes two crucial states in the detonation wave, i.e., the von Neumann (VN) spike, which corresponds to the shock wave that initiates chemical reactions in the explosive, and the Chapman-Jouguet (CJ) state, which occurs at the end of the reaction zone [24]. The pressure at the VN spike (P_{VN}), the pressure at the CJ state (simply called detonation pres-

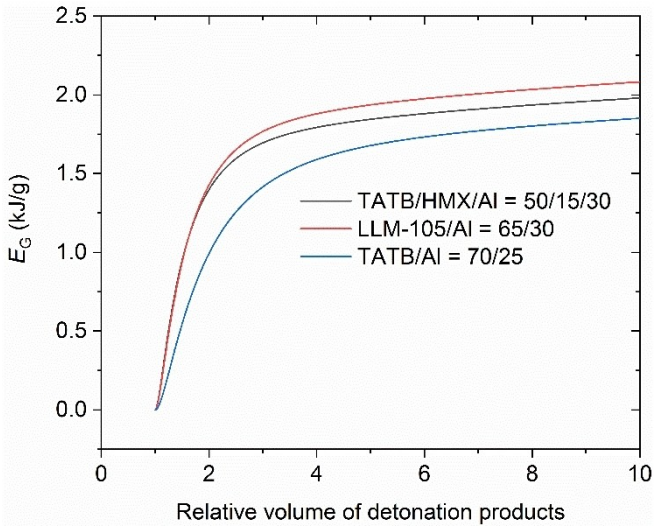

Figure 9. Variation of the Gurney energy with the relative volume of detonation products.

Table 3. Copper tube velocity and Gurney energy.

Explosive	ρ_0 (g/cm^3)	D (m/s)	u_L (m/s)	E_G (kJ/kg)
TATB/HMX/Al = 50/15/30	2.04	7493	1268	1984
LLM-105/Al = 65/30	2.01	7550	1302	2060
TATB/Al = 70/25	2.03	7224	–	1829

sure, P_{CJ}), reaction zone time (t_{CJ}), and length (X_{CJ}) are important parameters describing the process of detonation. The observation of shock wave properties in well-characterized inert material in contact with an explosive charge is widely used in the past few decades to assess the detonation reaction zone parameters.

Apparent interface velocity histories were obtained and corrected for the index of refraction of LiF to generate true interface velocity histories [25]. The corrected velocity profiles were smoothed and drawn in Figure 10. For all the aluminized explosives, the ZND detonation wave structure was observed: a discontinuous jump to maximum particle velocity at the detonation wave front followed by a rapid decrease to the CJ velocity as the chemical energy is released. Behind the CJ state, the slowly declining velocity profile corresponds to the expansion of reaction products (Taylor rarefaction wave), in which most micron-diameter aluminum particles react with detonation products [26]. However, the absence of a distinct inflection point, corresponding to the CJ point, in Figure 10 made it difficult to analyze the structure of the detonation wave directly. Therefore, the time history of $-du_p/dt$ is applied to determine the CJ point on the particle velocity profile. With allowance for the experimental error, the dependence of $-du_p/dt$ on t in semi-logarithmic coordinates is represented as two straight lines, and the second line has practically zero slopes ($du_p/dt \approx$ const) [27]. The point of intersection of these lines, which corresponds to the Jouguet plane, determines the reaction time t_{CJ} (the time of passage of the HE element from the front to the Jouguet plane) The time history of $-du_p/dt$ and two linear fits to the $-du_p/dt$ profile are presented in Figure 11. When t_{CJ} was determined, u_{pCJ} was read from the particle velocity profiles in Figure 10.

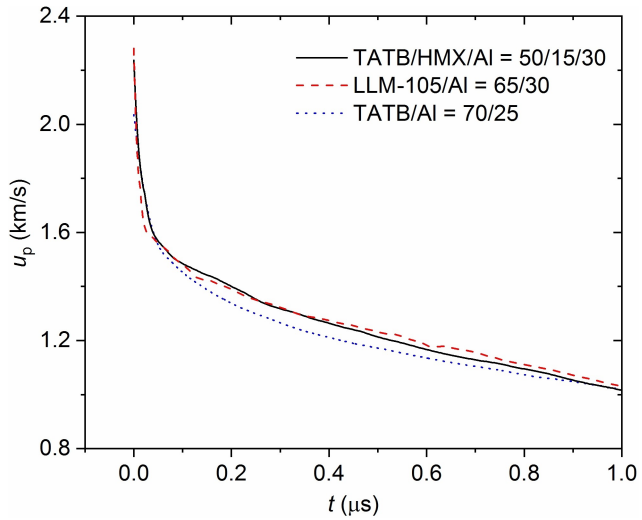

Figure 10. Interface particle velocity histories of samples.

LiF is an inert material with a higher shock impedance than the main charge, thus a strong shock is reflected back into the reacting explosive. Impedance analysis on the measured point at the explosive-window interface was conducted. Using the linear Hugoniot relationship of LiF, which is established from the experimental relationship between shock velocity U_s and particle velocity u_p as [28]

$$U_s = 5.201 + 1.323u_p. \tag{2}$$

Assuming consecutive velocity and pressure at the explosive/ window interface, the wave propagation was solved in the pressure-particle velocity plane as shown in Figure 12 for TATB/HMX/Al = 50/15/30. CJ point is the point of tangency of the detonation products Hugoniot and the detonation Rayleigh line. In Figure 12, the CJ point is at the intersection of the reflected products Hugoniot and the

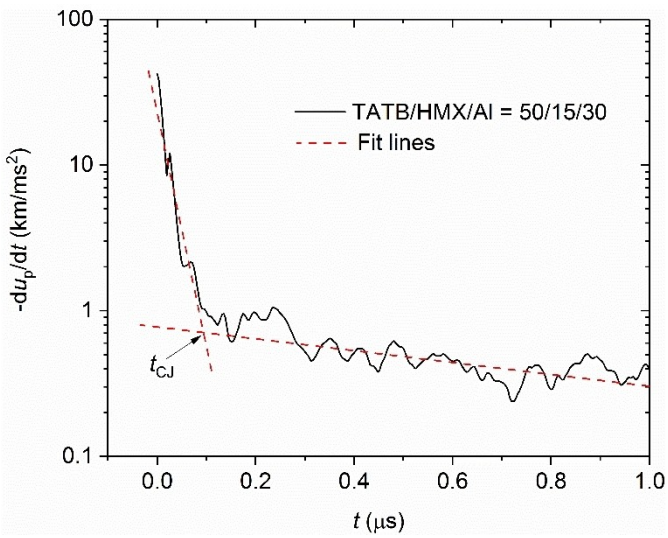

Figure 11. Time history of $-du_p/dt$ for TATB/HMX/Al = 50/15/30.

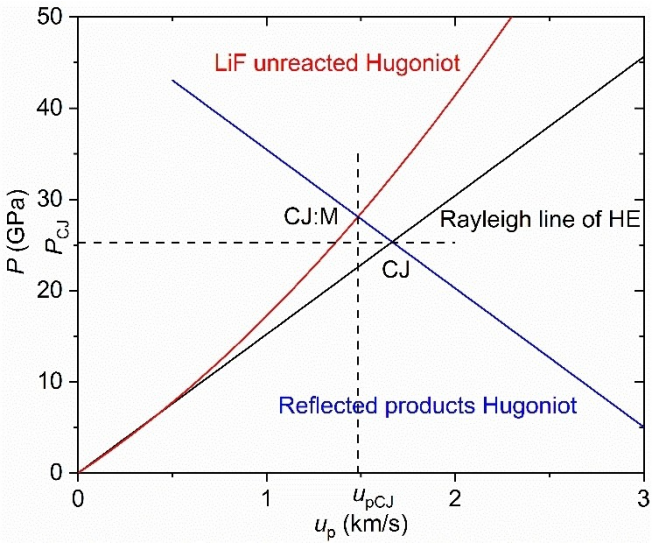

Figure 12. Impedance match plot of P_{CJ} for TATB/HMX/Al = 50/15/30.

Rayleigh line, where the reflected products Hugoniot was approximated as the reflected Rayleigh line. When the detonation shock wave spreads to the explosive/ window interface, a reflected shock wave will then propagate in the explosive. The interface states then become CJ:M as shown in the figure. The impedance match equation was then used to calculate the detonation pressure P_{CJ} as [29]

$$P_{CJ} = u_{pCJ}\ (\rho_{LiF} U_s + \rho_0 D)/2, \quad (3)$$

where u_{pCJ} is the interface particle velocity corresponding to CJ state, ρ_{LiF} is the initial density of LiF (2.64 g/cm^3), D and ρ_0 are given in Table 3. Moreover, the length of the reaction zone X_{CJ} could be calculated by the formula [27]

$$x_{CJ} = \int_0^{t_{CJ}} (D - u_p)\mathrm{d}t. \quad (4)$$

Table 4 lists the detonation reaction zone parameters of samples. The measurement uncertainty was ~5 %, which results from the accuracy of determining the CJ point, the correction of the interface velocity, and the approximation of the reflected products Hugoniot. The parameters in Table 4 show that LLM-105/Al = 65/30 has the highest detonation pressure and the shortest reaction zone time and length, while TATB/Al = 70/25 has the lowest detonation pressure and the longest reaction zone time and length.

4 Conclusions

Two new types of aluminized explosives were formulated as TATB/HMX/Al/fluorine resin and LLM-105/Al/fluorine resin. The thermal stability, mechanical sensitivity, and detonation performance were studied and compared with the thermally stable TATB/Al/fluorine resin explosives reported previously. The partial replacement of TATB by HMX and total replacement of TATB by LLM-105 significantly increase the heat of the explosion and two representative formulations of TATB/HMX/Al = 50/15/30 and LLM-105/Al = 65/30 were selected. The TGA/DSC and thermal cook-off tests show that the thermal stability of LLM-105/Al = 65/30 is better than that of TATB/HMX/Al = 50/15/30, but both of them are inferior to TATB/Al = 70/25. The impact sensitivity from high to low is LLM-105/Al = 65/30, TATB/HMX/Al = 50/15/30, and TATB/Al = 70/25. All of the samples are insensitive to friction. For detonation performance, both of the two new samples are superior to the formerly reported TATB/Al = 70/25, and LLM-105/Al = 65/30 exhibits the best performance that it has the highest Gurney energy, detonation velocity, and detonation pressure.

In summary, compared to the thermally stable and insensitive TATB/Al explosives, those two new types of aluminized explosives have improved detonation performance with the cost of thermal stability and impact sensitivity, but they still have acceptable thermal stability and mechanical sensitivity. Among them, LLM-105/Al is more attractive in that it shows a better balance between detonation performance and stability.

Table 4. Detonation reaction zone parameters.

Explosive	u_{pCJ} (m/s)	t_{CJ} (ns)	P_{CJ} (GPa)	X_{CJ} (mm)
TATB/HMX/Al = 50/15/30	1485	95	25.3	0.56
LLM-105/Al = 65/30	1507	82	25.7	0.48
TATB/Al = 70/25	1448	103	23.9	0.58

Acknowledgements

This research is supported by the National Natural Science Foundation of China (21875230) and the Innovation Project of Innovation and Development Foundation of CAEP (CX2019009). The authors wish to thank Qi Liu and Jichao Zan for their constructive advice.

Data Availability Statement

No data available.

References

[1] P. P. Vadhe, R. B. Pawar, R. K. Sinha, S. N. Asthana, A. Subhananda Rao, Cast aluminized explosives (review). *Combust. Explos. Shock Waves* **2008**, *44*, 461–477. doi: 10.1007/s10573-008-0073-2.

[2] W. A. Trzciński, S. Cudziło, L. Szymańczyk, Studies of Detonation Characteristics of Aluminum Enriched RDX Compositions. *Propellants Explos. Pyrotech.* **2007**, *32*, 392–400. doi: 10.1002/prep.200700201.

[3] L. Maiz, W. A. Trzciński, Detonation Characteristics of New Aluminized Enhanced Blast Composites. *Propellants Explos. Pyrotech.* **2018**, *43*, 650–656. doi: 10.1002/prep.201800094.

[4] W. Cao, Q. Song, D. Gao, Y. Han, S. Xu, X. Lu, X. Guo, Detonation Characteristics of an Aluminized Explosive Added with Boron and Magnesium Hydride. *Propellants Explos. Pyrotech.* **2019**, *44*, 1393–1399. doi: 10.1002/prep.201900164.

[5] A. Sikder, N. Sikder, A review of advanced high performance, insensitive and thermally stable energetic materials emerging for military and space applications. *J. Hazard. Mater.* **2004**, *112*, 1–15. doi: 10.1016/j.jhazmat.2004.04.003.

[6] S. F. Rice, *The unusual stability of TATB: a review of the scientific literature*, Report No. UCRL-LR-103683, Lawrence Livermore National Laboratory, Livermore, CA, USA **1990**.

[7] F. Gong, H. Guo, J. Zhang, C. Shen, C. Lin, C. Zeng, S. Liu, Highly Thermal Stable TATB-based Aluminized Explosives Realizing Optimized Balance between Thermal Stability and Detonation Performance. *Propellants Explos. Pyrotech.* **2017**, *42*, 1424–1430. doi: 10.1002/prep.201700206.

[8] J. P. Agrawal, Past, present & future of thermally stable explosives. *Cent. Eur. J. Energ. Mater.* **2012**, *9*, 273–290.

[9] P. Pagoria, A comparison of the structure, synthesis, and properties of insensitive energetic compounds. *Propellants Explos. Pyrotech.* **2016**, *41*, 452–469. doi: 10.1002/prep.201600032.

[10] Ł. Gutowski, S. Cudziło, Synthesis and properties of novel nitro-based thermally stable energetic compounds. *Def. Technol.* **2021**, *17*, 775–784. doi: 10.1016/j.dt.2020.05.008.
[11] P. F. Pagoria, *Synthesis, scale-up, and characterization of 2, 6-diamino-3, 5-dinitropyrazine-1-oxide (LLM-105)*, Report No. UCRL-JC-130518, Lawrence Livermore National Laboratory, Livermore, CA, USA **1998**.
[12] T. Tran, P. Pagoria, D. Hoffman, J. Cutting, R. Lee, R. Simpson, *Characterization of 2, 6-diamino-3, 5-dinitropyrazine-1-oxide (LLM-105) as an insensitive high explosive material*, Report No. UCRL-JC-147932, Lawrence Livermore National Laboratory, Livermore, CA, USA **2002**.
[13] P. Pagoria, M.-X. Zhang, N. Zuckerman, G. Lee, A. Mitchell, A. DeHope, A. Gash, C. Coon, P. Gallagher, Synthetic Studies of 2,6-Diamino-3,5-Dinitropyrazine- 1-Oxide (LLM-105) from Discovery to Multi-Kilogram Scale. *Propellants Explos. Pyrotech.* **2018**, *43*, 15–27. doi: 10.1002/prep.201700182.
[14] C. M. Tarver, P. A. Urtiew, T. D. Tran, Sensitivity of 2, 6-Diamino-3, 5-Dinitropyrazine-1-Oxide. *J. Energ. Mater.* **2005**, *23*, 183–203. doi: 10.1080/07370650591001853.
[15] B. Tan, X. Long, R. Peng, H. Li, B. Jin, S. Chu, On the shock sensitivity of explosive compounds with small-scale gap test. *J. Phys. Chem. A* **2011**, *115*, 10610–10616. doi: 10.1021/jp204814f.
[16] W. Xu, C. An, J. Wang, J. Dong, X. Geng, Preparation and Properties of An Insensitive Booster Explosive Based on LLM-105. *Propellants Explos. Pyrotech.* **2013**, *38*, 136–141. doi: 10.1002/prep.201100099.
[17] J. Zhang, P. Wu, Z. Yang, B. Gao, J. Zhang, P. Wang, F. Nie, L. Liao, Preparation and Properties of Submicrometer-Sized LLM-105 via Spray-Crystallization Method. *Propellants Explos. Pyrotech.* **2014**, *39*, 653–657. doi: 10.1002/prep.201300174.
[18] D. M. Williamson, S. Gymer, N. E. Taylor, S. M. Walley, A. P. Jardine, A. Glauser, S. French, S. Wortley, Characterisation of the impact response of energetic materials: observation of a low-level reaction in 2, 6-diamino-3, 5-dinitropyrazine-1-oxide (LLM-105). *RSC Adv.* **2016**, *6*, 27896–27900. doi: 10.1039/C6RA03096 C.
[19] United Nations, UN Recommendations on the Transport of Dangerous Goods, Manual and Tests and Criteria, 7th revised edition, United Nations Publication, New York and Geneva **2019**.
[20] W. A. Trzciński, L. Szymańczyk, B. Kramarczyk, Determination of the Equation of State for the Detonation Products of Emulsion Explosives. *Cent. Eur. J. Energ. Mater.* **2019**, *16*, 49–64. doi: 10.22211/cejem/104684.
[21] J. Kimura, N. Kubota, Thermal decomposition process of HMX. *Propellants Explos. Pyrotech.* **1980**, *5*, 1–8. doi: 10.1002/prep.19800050102.
[22] H. Li, B. Cheng, S. Liu, F. Nie, J. Li, Recrystallization and Properties of LLM-105. *Chin. J. Energ. Mater.* **2008**, *16*, 686–688.
[23] H. Hornberg, Determination of Fume State Parameters from Expansion Measurements of Metal Tubes. *Propellants Explos. Pyrotech.* **1986**, *11*, 23–31. doi: 10.1002/prep.19860110106.
[24] J. Pachman, M. Künzel, O. Němec, J. Majzlík, A comparison of methods for detonation pressure measurement. *Shock Waves* **2018**, *28*, 217–225. doi: 10.1007/s00193-017-0761-5.
[25] P. A. Rigg, M. D. Knudson, R. J. Scharff, R. S. Hixson, Determining the refractive index of shocked [100] lithium fluoride to the limit of transmissibility. *J. Appl. Phys.* **2014**, *116*, 033515. doi: 10.1063/1.4890714.
[26] C. E. Needham, *Blast waves*, Springer, New York **2010**, p. 356.
[27] B. G. Loboiko, S. N. Lubyatinsky, Reaction Zones of Detonating Solid Explosives. *Combust. Explos. Shock Waves* **2000**, *36*, 716–733. doi: 10.1023/a:1002898505288.
[28] Q. Liu, X. Zhou, X. Zeng, S. N. Luo, Sound velocity, equation of state, temperature and melting of LiF single crystals under shock compression. *J. Appl. Phys.* **2015**, *117*, 045901. doi: 10.1063/1.4906558.
[29] J. K. Rigdon, I. B. Akst, An analysis of the "aquarium technique" as a precision detonation pressure measurement gage, *5th Symposium (International) on Detonation*, August 18–21, **1970**, Pasadena, CA, USA, 59–66.

Manuscript received: February 12, 2021
Revised manuscript received: June 17, 2021
Version of record online: July 6, 2021

